

Heterogeneous Interaction of Peroxyacetyl Nitrate on Liquid Sulfuric Acid

Renyi Zhang and Ming-Taun L  u

Earth and Space Sciences Division

Jet Propulsion Laboratory

California Institute of Technology

Pasadena, California 91109

Abstract

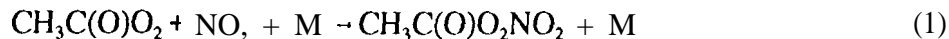
The uptake of peroxyacetyl nitrate (PAN) on liquid sulfuric acid surfaces has been investigated using a fast-flow reactor coupled to a chemical ionization mass spectrometer. PAN was observed to be reversibly adsorbed on sulfuric acid. From the time-dependent uptake, Henry's law volatility constant of PAN in sulfuric acid was obtained. The measured volatility constant was found to depend strongly on temperature (199-226 K), but weakly on acid composition (46-72 wt %). On 72 wt % H_2SO_4 , for example, the effective Henry's law volatility constant was determined to be about 5.6×10^4 and $3.1 \times 10^3 \text{ M atm}^{-1}$ at 208 and 222 K, respectively. Heterogeneous reactions of PAN with HCl, Cl, ClO, and OClO on liquid sulfuric acid were also investigated and found to be very slow ($\gamma < 1 \times 10^{-4}$). Atmospheric implications of the present results are discussed.

(Submitted to *J. Geophys. Res. Atmosphere*, Sept. 1996)

Introduction

The atmospheric chemistry of nitrogen compounds plays an important role in photochemical oxidation processes that determine the final forms of atmospheric pollutants. Although these photochemical reactions ultimately lead to the conversion of nitrogen oxides (NO_x) into HNO_3 , there are also a number of side reactions that produce a variety of organic nitrates [Darnall et al., 1976; Atkinson et al., 1982; Atkinson and Lloyd, 1984; Calvert and Madronich, 1987]. These organic nitrates act as temporary reservoirs of reactive nitrogen, which can be redistributed throughout the atmosphere by circulations [Singh and Hansel, 1981] and, thus, provide a source of NO_x in clean atmosphere where it is critical to the oxidation of hydrocarbons and the formation of ozone.

Peroxyacetyl nitrate ($\text{CH}_3\text{C}(\text{O})\text{O}_2\text{NO}_2$, PAN) is recognized as one of the most abundant tropospheric organic nitrates. Laboratory [Spicer et al., 1981; Akimoto et al., 1980] and field [Stephens et al., 1956; Singh et al., 1990; Ridley et al., 1990] studies have established that PAN can account for a significant fraction of reacted NO_x ; it has been detected globally from ground level to an altitude of 10 km [Singh et al., 1986; Singh et al., 1992] at concentrations that are significant relative to the total NO_y budget [Kasting and Singh, 1986; Derwent and Jenkin, 1991; Honrath and Jaffe, 1992; Parrish et al., 1992; Stepson et al., 1992; Kasibhatla et al., 1993]. In the atmosphere, PAN is formed primarily from photochemical reactions of a wide variety of small nonmethane hydrocarbons in the presence of NO_x via the reaction of peroxyacetyl radicals with NO_2 ,



The fate of PAN is determined by several atmospheric removal processes, including thermal decomposition, UV photolysis, and chemical reactions with OH or Cl. In the lower atmosphere, the concentration of PAN is mainly controlled by thermal decomposition, which is strongly temperature dependent [Orlando et al., 1992; Roberts and Bertman, 1992; Grosjean et al., 1994]. At higher altitudes (> 7 km) where the thermal decomposition is slow, photolysis becomes the dominant sink for PAN [Mazely et al., 1995; Talukdar et al., 1995].

Another potential loss mechanism of PAN in the atmosphere is its interaction with particulate. PAN may influence precipitation quality directly by contributing additional nitrate,

and it may also have an indirect effect by serving as an oxidizing agent in aqueous solutions, perhaps in a manner similar to that of hydrogen peroxide. For example, in alkaline solutions PAN has been found to rapidly hydrolyze and yield nitrite and acetate anions and molecular oxygen [Nicksic, 1967; Stephens, 1969]. A number of authors have reported volatility and hydrolysis of PAN in distilled and sea water and slightly acidic solutions at or near room temperature [Holdren, et al., 1984; Lee, 1984; Kames et al., 1991; Langer, et al., 1992; Kames and Schurath, 1995]. These studies suggest that PAN is soluble in these aqueous solutions (the Henry's law volatility constant is about 4 M atm^{-1} at 293 K), but its hydrolysis rate is very low. In addition, Lee [1984] investigated the oxidizing effect of O_2 , O_3 , and H_2O_2 in aqueous PAN solutions and suggested that PAN is not a good oxidant in cloud water.

A recent study [Jaegle et al., 1996] has proposed that an observed chlorine deficit in the lower stratosphere on the basis of field measurements may be accountable due to the formation of oxo acids (such as HClO_2 , HClO_3 , or HClO_4) from heterogeneous reactions of chlorine oxides (such as ClO or OClO) with sulfate aerosols. Our results [Zhang and L  u, 1996, unpublished results] indicate that formation of these oxo acids from direct uptake of chlorine oxides on sulfuric acid is unlikely, but a possible oxidation mechanism may involve heterogeneous interactions of some chlorine containing species in the presence of a strong oxidizing agent such as PAN in sulfuric acid.

Although it generally has been concluded that PAN does not contribute significantly to the acidification of cloud or fog particles, and that its loss from the atmosphere by wet deposition is slow, heterogeneous chemistry of PAN on sulfate aerosols at low temperatures is still unexplored. This information is needed for a thorough understanding of the reservoir species for NO_x and the conditions under which these reservoirs act to initiate photochemical processes. In this article, we describe a laboratory study of heterogeneous interaction of PAN with liquid sulfuric acid at conditions representative of the upper troposphere and lower stratosphere, i.e. in the temperature range of 199-226 K and with H_2SO_4 contents of 46-72 wt %. From the gas-phase kinetic data, the Henry's law volatility constant of PAN in H_2SO_4 is determined. In addition, we report measurements of oxidation potential of PAN in sulfuric acid for species such as HCl and some chlorine oxides. Finally, atmospheric implications of the present results will be addressed.

Experimental

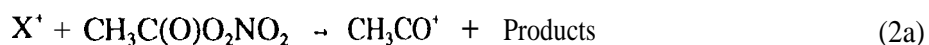
PAN uptake measurements were conducted in a fast-flow reactor coupled to a chemical ionization mass spectrometer (CIMS). Detailed descriptions of the experimental apparatus and procedures have been given elsewhere [Zhang et al., 1994; Leu et al., 1995; Zhang et al., 1996], and only a brief overview is presented here along with features pertinent to this work.

The borosilicate flow reactor which had an inner diameter of 2.8 cm and an overall length of 60 cm was horizontal] y-mounted and temperature regulated. Liquid H_2SO_4 films were prepared by totally covering the inside wall of the flow tube with sulfuric acid solutions. At low temperatures (< 220 K) the solutions were sufficiently viscous to produce essentially a static film which lasted over the time scale of the experiments. The thickness of the films was estimated to be about 0.1 mm, based on the amount of acid solution used and the geometric area covered. Composition of the liquid H_2SO_4 was governed by the temperature and H_2O partial pressure in the flow tube [Zhang et al., 1993]: once exposed to H_2O vapor, the sulfuric acid film took up H_2O and became more diluted until equilibrium was reached. H_2O vapor was admitted to the flow tube with the main He carrier gas. The partial pressure of H_2O was estimated by passing a known flow of He carrier gas through an H_2O reservoir at room temperature. It was controlled by diluting the humidified He flow (assuming 100% RH) with a dry He flow. During a warming/cooling process, the amount of water introduced into the flow reactor was adjusted to compensate for possible changes in the acid composition of the liquid film, incurred due to the changing temperature. The error limit for estimating the acid composition of the films was about 1-2 wt %, considering uncertainties associated with temperature (± 1 K) and water partial pressure (± 20 %) measurements. In addition, some uptake measurements of PAN were performed by directly preparing sulfuric acid of known composition (determined by weighing a known volume of the solution and using its specific gravity with an estimated uncertainty in the acid content of about ± 0.5 wt %) on the inner wall of the flow reactor. For these experiments, water vapor was also added to the flow reactor in order to prevent evaporation of water from the liquid film and subsequent change in the acid composition. The results obtained using these two methods were found to be consistent within the experimental uncertainty.

PAN was synthesized from the reaction of peracetic acid and concentrated nitric

acid/sulfuric acid in the solvent n-tridecane ($C_{13}H_{28}$), according to the method of Gaffney et al. [1984]. The reaction mixture was then washed several times at 273 K in order to remove water soluble impurities. The PAN sample was collected by passing the vapor from the tridecane solution through a reservoir immersed in a liquid nitrogen dewar. Infrared spectra taken from the gaseous samples showed that the fraction of PAN in the vapor was greater than 98%; the identification of PAN was made from the appearance of five stronger bands located at 793, 1163, 1302, 1741, and 1841 cm^{-1} , consistent with previous studies [Kleindienst, 1994]. The high purity of the PAN sample was further confirmed by mass spectrometric measurements. During the experiment the solution containing PAN was maintained at temperatures between 210 and 220 K. Gaseous PAN was added to the flow tube along with a small He flow ($0.1-10.0\text{ cm}^3\text{ min}^{-1}$ at STP) and further diluted in the main He flow ($310\text{ cm}^3\text{ min}^{-1}$ at STP) before contacting the liquid acid surface. The concentrations of PAN in the neutral flow reactor were determined according to the vapor pressure expression of $\ln P(\text{Torr}) = -4586/7 + 18.77$ for pure PAN in the temperature range of 210-330 K [Kleindienst, 1994] and the dilution factor of the PAN carrier flow. A 3-way switching valve was designed to quickly change the PAN flow either downstream or upstream (i.e., to expose or bypass PAN vapor to sulfuric acid), with a delay time shorter than 50 milliseconds. Typically, the flow tube was operated at a pressure of 0.40 to 0.45 Torr, with an average flow velocity ranging from 1600 to 2000 $cm\text{ s}^{-1}$.

PAN was detected by the CIMS operated at a positive ion detection mode. We have used the following ion-molecular reaction as the detection scheme for PAN,



where the reagent ion X^+ can be He^+ , H_3O^+ , or O_2^+ . Reaction 2 has not been previously studied; however, it is expected to be exothermic [Harrison, 1992]. Figure 1d illustrates the mass spectra of PAN after reaction with the O_2^+ reagent ion. The peaks at $m/e = 43$ and 46 arise from the CH_3CO^+ and NO_2^+ ions, respectively. To generate the positive reactant ions, a large flow of helium 6-10 slpm (standard liter per minute at 293 K) was first passed through a rhenium filament (6-10 A emission current) in the ion flow tube, forming He^+ ions by electron impact ionization (Fig. 1a). It was found that even a small fraction of water in the helium supply could result in a complete loss of the He^+ ions due to the formation of hydronium ions. As a result, the

helium flow was circulated through a liquid nitrogen trap prior to entering the ion flow tube, in order to remove water. Subsequently, O_2^+ or H_3O^+ ions were produced by addition of a small amount of O_2 or H_2O (about a few $cm^3 min^{-1}$ at STP) downstream of the ion flow tube to react with the He^+ ions (Figs. 1 b and 1c),



or



The advantage of using the O_2^+ reagent ion was due to its very small rate for the reaction with H_2O ($< 1 \times 10^{12} cm^3 s^{-1}$) [Anicich, 1994], so that the PAN detection was not affected by the variation of water concentration in the neutral flow reactor. For the majority of experiments reported here, PAN was detected at $m/e = 43$ (corresponding to the CH_3CO^+ ion) using the O_2^+ reagent ion, but the results did not vary with the various reagent ions used. Typical PAN concentrate ions used in the present study were about 3×10^9 to 3×10^{10} molecules cm^{-3} in the neutral flow reactor. The lower reactant concentrations used in this experiment were essential to minimize the occurrence of secondary reactions. Detection sensitivity of PAN in the CIMS was estimated to be about 1×10^8 molecules cm^{-3} with a S/N ratio of unity for 1 s integration time.

Unlike PAN, detection for HCl, Cl, ClO, and OClO was made using the negative reagent ion SF_6^- ; they were monitored as $F \bullet HCl$, Cl^- , ClO^- , and $OClO^-$, respectively. Atomic chlorine was produced by passing a helium flow (about $150 cm^3 s^{-1}$ at STP) with a trace of Cl_2 through a microwave discharge. OClO was generated by flowing a Cl_2/He mixture through a glass column packed with $NaClO_2$ powders. ClO radicals were formed by the reaction of chlorine atoms with chlorine dioxide. The concentrations of these species in the neutral flow reactor were estimated by assuming the same rate coefficient of these species with SF_6^- as that of HCl with SF_6^- ($\sim 1 \times 10^{-9}$ molecules $cm^3 s^{-1}$) [Huey et al., 1995] and comparing their relative intensities with respect to HCl under similar conditions. The CIMS was calibrated for HCl by measuring the flow rate of a known mixture of HCl in He; the calibration procedure was described in detail in our previous work [Zhang et al., 1994; Zhang et al., 1996]. Detection sensitivity of these species was similar to that of PAN described above. Ion chemistry was also explored for perchloric acid by preparing its pure sample. $HClO_4$ was synthesized by slowly adding concentrated H_2SO_4 (~ 96

wt %) into KClO_4 powders at room temperature and collecting the vapor at the liquid nitrogen temperature. HClO_4 was detected using the negative reagent ion SF_6^- and monitored as ClO_4^- .

Product ions in the ion flow reactor were effused through an orifice, of 0.5 mm diameter, which was biased at a small voltage (1-10 V), and further collimated by a set of lenses. The ions were then mass selected by a differentially pumped mass spectrometer and detected by a channeltron electron multiplier operated in an analog mode. The CIMS detector was linear over the range of PAN concentrations used, since the concentrations of reactant ion were not affected by the small concentration of the neutral reactant,

In general, gas-phase uptake by a planar liquid surface is due to either time-dependent physical adsorption or irreversible chemical reaction, which can be treated by a diffusive and reaction equation [see, for example, Danckwerts, 1970],

$$\frac{\partial C}{\partial t} = D_l \frac{\partial^2 C}{\partial x^2} - R_l \quad (6)$$

where C represents the concentration of the species in the liquid, x is the distance, D_l is the liquid-phase diffusion coefficient, and R_l is the rate of liquid phase reaction. For the case where there is no chemical loss in a semi-infinite planar liquid (i.e. $R_l = 0$), eq. 6 has been solved as [Danckwerts, 1951],

$$\gamma_{obs}(t) = \alpha [1 - \text{erf}(h\sqrt{D_l t})] e^{h^2 D_l t} \quad (7)$$

where $h = \alpha \omega / (4 R T H^*)$, α is the mass accommodation coefficient, ω is the mean thermal speed of the molecule, R is the gas constant ($0.082 \text{ L atm}^{-1} \text{ mol}^{-1} \text{ K}^{-1}$), T is the temperature, H^* is the effective Henry's law solubility constant, and $\text{erf}(x)$ is the Gauss error function. Under the condition that $h\sqrt{D_l t} \gg 1$ (lower solubility or longer time), this solution can be approximated as [Hanson and Ravishankara, 1993; Abbatt, 1995; Kolb et al., 1995]

$$\gamma_{obs}(t) = \frac{4 R T H^* D_l}{\omega} \left(\frac{1}{\pi t} \right)^{\frac{1}{2}} \quad (8)$$

Hence, eq. 8 relates the measured time-dependent uptake coefficient (γ_{obs}) to the product of the effective Henry's law solubility constant and the square root of the liquid-phase diffusion coefficient ($H^* \sqrt{D_l}$). Since the thickness of liquid sulfuric acid films (l) used in the present study was finite, eq. 8 applies only when $1 \gg l_d$, where l_d ($l_d = (\pi D_l t)^{1/2}$) is the characteristic depth of

liquid-phase diffusion at time t . Under our laboratory conditions, the thickness of sulfuric acid films was estimated to be about 0.1 mm (or 100 μm) and the typical exposure time for PAN uptake was less than 1 min (see Figure 2). The depth of liquid-phase diffusion was calculated to be less than 20 μm using a diffusion coefficient of $1 \times 10^{-8} \text{ cm}^2 \text{ s}^{-1}$, so that the above condition held reasonably well. The uptake coefficient can be calculated from [Motz and Wise, 1960]

$$\gamma_{\text{obs}}(t) = \frac{2rk}{\omega + rk} \quad (9)$$

where r is the radius of the flow reactor. The first-order rate coefficient (k) is related to the fractional change ($\Delta n/n$) in the gas-phase concentrations of PAN before and after exposure to liquid sulfuric acid by

$$k \approx \frac{2F_g}{rA} \frac{\Delta n}{n} \quad (10)$$

where F_g is the carrier gas volume rate of flow ($\text{cm}^3 \text{ s}^{-1}$) and A is the surface area of exposed liquid. When the uptake rate became gas-phase diffusion limited, the first-order rate coefficient was corrected for gas-phase diffusion restrictions according to the method suggested by Brown [1978]. The gas-phase diffusion coefficient for PAN in He was estimated to be $PD_g = 168 \text{ Torr cm}^2 \text{ s}^{-1}$ at 230 K, with a temperature dependence of $T^{1.75}$ [Marrero and Mason, 1972]. From the time evolution of the PAN signal, the quantity $H^* \sqrt{D_l}$ can be extracted from the slope of a plot of $\gamma_{\text{obs}}(t)$ versus $t^{-1/2}$, according to eq. 8.

To estimate the liquid-phase diffusion coefficient, we adopted a cubic cell model that was initially developed for self-diffusion in liquids [Houghton, 1964; Luo et al., 1994],

$$D_l = \frac{RT\rho\lambda^2}{6\eta M_{\text{PAN}}} \quad (11)$$

and

$$\lambda = \frac{1}{2} \left(d + \left[\frac{xM_{\text{SO}_4^{2-}} + (1-x)M_{\text{H}_2\text{O}}}{\rho} \right]^{1/3} \right) \quad (12)$$

where ρ is the density of liquid H_2SO_4 and x is the H_2SO_4 mole fraction. M_{PAN} , $M_{\text{SO}_4^{2-}}$, and $M_{\text{H}_2\text{O}}$ are the molecular weights of PAN, SO_4^{2-} , and H_2O respectively. Assuming that there is no

liquid-phase dissociation, we estimated an effective molecular dimension (d) of $\sim 6.3 \text{ \AA}$ for PAN diffusing in liquid sulfuric acid. The viscosity coefficient (η) of sulfuric acid, used in eq. 11, incorporated the viscosity measurements by Williams and Long [1995],

Results and Discussion

PAN Uptake and Volubility Measurements

To study the time-dependent uptake, a PAN flow, which bypassed a liquid sulfuric acid film, was first established. When a steady PAN signal was obtained, the direction of the PAN flow was quickly changed from downstream to upstream via a 3-way switching valve, exposing a 20-30 cm length of the acid film to PAN vapor. The PAN signal was continuously monitored using the CIMS and uptake from the gas phase was determined from the decline and recovery in the PAN signal. Thus, changes in the mass spectrometer signal that occurred when PAN was exposed to a sulfuric acid film reflected the net flux that PAN was lost to the surface [Worsnop et al., 1989].

Figure 2 shows a typical example of the temporal profile of PAN as it was exposed and bypassed a 30-cm length of a liquid sulfuric acid film at 212 K. The acid content of the film was estimated to be about 59 wt %, Figure 2 shows that the PAN concentration in the gas phase fell instantly upon exposure to liquid H_2SO_4 at about 1.2 min, because of rapid uptake into the film, which was initially free of PAN. The signal later recovered, as the film became saturated and started to evaporate some of the PAN which had been dissolved, and, asymptotically approached its original value. Switching the PAN flow downstream at 3.4 min resulted in an opposite peak due to resorption. The shapes of the adsorption and resorption curves were nearly identical, suggesting that PAN was physically taken up by liquid sulfuric acid without undergoing irreversible aqueous phase reactions. This held true over the entire H_2SO_4 content and temperature ranges investigated, i.e., over H_2SO_4 contents of 46-72 wt % and temperatures of 199-226 K. Under no circumstances did we observe any gaseous products by the CIMS associated with PAN uptake in sulfuric acid.

The data displayed in Figure 2 were analyzed by calculating the uptake coefficient using

eq. 9 from the initial and time-dependent signals of PAN, Figure 3 plots the time-dependent uptake coefficient as a function of $t^{1/2}$, yielding a straight line in accord with eq. 8. The uptake coefficient is initially about 0.008 and its value decreases rapidly with time, indicating that at longer times the decreasing uptake coefficient is a manifestation of the volatility limitation. The slope of the straight line in Figure 3 is proportional to the quantity $H^* \sqrt{D_l}$; a value of $2.7 \text{ M atm}^{-1} \text{ cm}^2 \text{ s}^{-1/2}$ is obtained in this case,

The measured quantity $H^* \sqrt{D_l}$ on sulfuric acid is summarized in Figure 4. These measurements were performed at temperatures between 199 and 226 K and with acid contents between 46 and 72 wt %. The different symbols represent various acid compositions used. Figure 4 shows that the quantity $H^* \sqrt{D_l}$ increases markedly with decreasing temperatures. This is expected since physical volatility in general increases with decreasing temperatures. On the other hand, the quantity $H^* \sqrt{D_l}$ varies slightly with acid composition at a given temperature. The estimated uncertainty in these measurements is about $\pm 50 \%$, including systematic errors in the measurements and random errors in the data.

Effective Henry's volatility constants for data displayed in Figure 5 were determined by estimating the liquid-phase diffusion coefficient D_l of corresponding temperatures and acid compositions using eq. 11. Obtained values of H^* for PAN on sulfuric acid of various contents are plotted against the reciprocal of temperature in Figure 5. Also shown in the figure as the dashed line is the Henry's law volatility constants extrapolated to low temperatures based on the work of Kames et al. [1991] and Kames and Schurath [1995]. These authors reported Henry's law solubility constants measured at temperatures between 273 and 293 K and found very little pH dependence for this quantity in the range of $3.2 < \text{pH} \leq 6.7$. Figure 5 indicates that the effective Henry's volatility constant of PAN in sulfuric acid depends strongly on temperature, but weakly on acid content. At a given temperature, the values for 72 wt % sulfuric acid are about a factor of two or three larger than those measured on more dilute sulfuric acid solutions. The slightly higher H^* values in concentrated sulfuric acid occurs because the measured quantity $H^* \sqrt{D_l}$ does not change appreciably with the acid composition (Figure 4), but the liquid-phase diffusion coefficient decreases drastically with increasing acid content, because of increasing viscosity. Nevertheless, in most cases, our measured H^* values agree reasonably well with the extrapolated

values from the literature data within a factor of two, except for 72 wt % H_2SO_4 , in which case the maximum difference is about a factor of five. For a given acid composition, the temperature dependence of the effective Henry's law constant is expressed by $\ln H^* = -A H/RT + A S/R$, where ΔH and ΔS are the changes of enthalpy and entropy associated with the PAN solvation. The values of ΔH derived from the present study vary from -12.0 to -18.7 kcal mol⁻¹, in the acid content range of 46 to 72 wt %; our value for ΔH in 46 wt % H_2SO_4 is similar to -11.8 kcal mol⁻¹ reported by Lee [1984] in aqueous solutions at temperatures between 283 and 295 K. The changes in entropy, ΔS , also vary from -38.2 to -68.0 cal mol⁻¹ K⁻¹ in the same acid composition range. Results of the measured values of $H^* \sqrt{D_l}$ and H^* for PAN in liquid sulfuric acid are summarized in Table 1.

in general, the effective Henry's law solubility constant H^* exceeds the physical Henry's law volatility constant H due to processes such as dissociation or chemical reactions proceeding in the aqueous phase [Schwartz, 1986]. The extent of acid-based dissociation for species such as HCl and HNO_3 in sulfuric acid increases with decreasing sulfuric acid content at a given temperature [Watson et al., 1990; Zhang et al., 1993] and, accordingly, their effective Henry's law constant increases with decreasing sulfuric acid content. One possible aqueous phase reaction for PAN has been proposed by Lee [1984],



At room temperature, the measured hydrolysis rate is too low to account for any measurable changes in the effective Henry's solubility constant [Lee, 1984; Kames et al., 1991; Kames and Schurath, 1995]. Likewise, the presently observed weak dependence of H^* with acid content reflects a lack of aqueous processes for PAN in sulfuric acid at low temperatures.

Heterogeneous Reactions of PAN with HCl, Cl, ClO, and OClO

We have investigated heterogeneous reactions of PAN with HCl, Cl, ClO, or OClO on sulfuric acid. The experiments were carried out by first allowing the H_2SO_4 film to equilibrate with PAN introduced from the gas phase and then measuring the uptake of HCl, Cl, ClO, or OClO. Partial pressures of these reactant species were maintained in the range of 1×10^{-6} to 1×10^{-7}

Torr with PAN slightly in excess ($\sim 3 \times 10^{-6}$ '1'err). For measurements with three acid compositions (42, 51, and 69 wt %) at temperatures of 202 and 224 K, we did not observe enhanced uptake coefficients of these species due to the presence of PAN in sulfuric acid. An upper limit of 1×10^{-4} can be placed for the reaction probability of PAN reactions with HCl, Cl, ClO, and OClO, based on our experimental conditions. Also, we performed two experiments by exposing HCl, Cl, ClO, or OClO vapor to sulfuric acid films (42 and 69 wt %) for 10 to 20 min at 210 K and then measuring PAN uptake. The partial pressure of PAN ($\sim 5 \times 10^{-7}$ Torr) was slightly less than that of HCl, Cl, ClO, or OClO (between about 1×10^{-6} and 3×10^{-6} '1'err). Similarly, no measurable enhancement in the PAN uptake coefficient was observed. Again, an upper limit of 1×10^{-4} was determined. Additionally, some experiments were performed by co-exposing PAN and one of the species HCl, Cl, ClO, or OClO to a sulfuric acid film of 42 wt % for 10 to 20 min at 210 K and then identifying the constituents in the liquid using the temperature-programmed-desorption method. No reaction product was identified; in particular, we observed no formation of any of the oxo acids of chlorine. Thus, we conclude that these reactions are of negligibly atmospheric importance on sulfate aerosols.

Conclusions

In this paper we have reported the first laboratory measurements of the interaction of PAN vapor with liquid sulfuric acid at conditions representative of the upper troposphere and lower stratosphere. PAN was observed to be physically taken up by sulfuric acid, without undergoing irreversible chemical reactions. The uptake data show that PAN is soluble in liquid sulfuric acid: the measured Henry's law volatility depends strongly on temperature, but weakly on sulfuric acid content. For 72 wt % H_2SO_4 , for example, the effective Henry's law constant of PAN was determined to be about $3.1 \times 10^3 \text{ M atm}^{-1}$ at 222 K and $5.6 \times 10^4 \text{ M atm}^{-1}$ at 208 K. Using the expression of $[\text{PAN(aerosol)}]/[\text{PAN(gas)}] = H^*L/RT$, the distribution of PAN between the gas and the condensed phases is estimated to be less than 10^{-6} , for a volume ratio (L) of 10^{-1} for sulfate aerosols (~ 70 wt %), at 220 K. Therefore, in the clean troposphere direct contribution to particulate nitrate levels by PAN dissolution in sulfate aerosols is probably not significant. Heterogeneous reactions between PAN and gas-phase species such as HCl, Cl, ClO, and OClO

were concluded to be unimportant on sulfate aerosols in the atmosphere.

Acknowledgements

The research was performed at the Jet Propulsion Laboratory (JPL), California Institute of Technology, under a contract with the National Aeronautics and Space Administration (NASA). We thank C. Miller for assistance in collecting IR spectra of PAN. Helpful discussions with several members of the JPL Kinetics and Photochemistry group are greatly acknowledged.

References

- Abbatt, J. P. D., interactions of HBr, HCl, and HOBr with supercooled sulfuric acid of stratospheric composition, *J. Geophys. Res.*, 100, 14,009-14,017, 1995.
- Akimoto, H., et al., Photooxidation of the propylene-NO_x-air system studies by long path Fourier transform infrared spectrometry, *Envir. Sci Technol.*, 14, 172-178, 1980.
- Anicich, V. G., Evaluated bimolecular ion-molecule gas phase kinetics of positive ions for use in modeling the chemistry of planetary atmospheres, cometary comae, and interstellar clouds, *J. Phys. Chem. Ref. Data*, 22, 1469-1569, 1994.
- Atkinson, R., et al., Alkyl nitrate formation from the NO_x-air photo-oxidation of C₂-C₈ alkanes, *J. Phys. Chem.*, 86, 4563-4569, 1982.
- Atkinson, R., and A.C. Lloyd, Evaluation of kinetic and mechanistic data from modeling of photochemical smog, *J. Phys. Chem. Ref. Data*, 13, 314-444, 1984.
- Brown, R. L., Tubular flow reactors with first order kinetics, *J. Res. Natl. Bur. Stand. (U.S.)*, 83, 1-8, 1978.
- Calvert, J.G, and S. Madronich, Theoretical study of the initial products of the atmospheric oxidation of hydrocarbons, *J. Geophys. Res.*, 92, 2211-2220, 1987.
- Danckwerts, P. V., Adsorption of simultaneous diffusion and chemical reaction into particles of various shapes and into falling drops, *Trans. Faraday Soc.*, 47, 1014-1023, 1951.
- Danckwerts, P. V., *Gas-Liquid Reactions*, McGraw-Hill, New York, 1970.
- Darnall, K. R., et al., Importance of RO₂ + NO in alkyl nitrate formation from C₄-C₆ alkane oxidations under simulated atmospheric conditions, *J. Phys. Chem.*, 80, 1948-1950, 1976.
- Derwent, R. G., and M.E. Jenkin, Hydrocarbons and the long-range transport of ozone and PAN across Europe, *Atmos. Environ.*, 25A, 1161-1178, 1991.
- Gaffney, J. S., R. Fajer, and G.I. Senum, An improved procedure for high purity gaseous peroxyacetyl nitrate production: Use of heavy lipid solvents, *Atmos. Environ.*, 18, 215-218, 1984.
- Grosjean, D., E. Grosjean, and E.L. Williams, Thermal-decomposition of PAN, PPN, and, vinyl-PAN, *J. Air Waste Manage.*, 44, 391-396, 1994.
- Hanson, D. R., and A.R. Ravishankara, Uptake of HCl and HOCl onto sulfuric acid: Solubilities, diffusivities, and reaction, *J. Phys. Chem.*, 97, 12,309-12,319, 1993.

- Harrison, A. G., *Chemical ionization mass spectrometry*, 2nd ed., CRC Press, Boca Raton, FL, 1992.
- Holdren, M. W., C.W. Spicer, and J.M. Hales, Peroxyacetyl nitrate volatility and deposition rate in acidic water, *Atmos. Environ.*, **18**, 1171-1173, 1984.
- Honrath, R. E., and D.A. Jaffe, The seasonal cycle of nitrogen-oxides in the Arctic troposphere at Barrow, Alaska, *J. Geophys. Res.*, **97**, 20,615-20,630, 1992.
- Houghton, G., Cubic cell model for self-diffusion in liquids, *J. Chem. Phys.*, **40**, 1628-1631, 1964.
- Huey, L. G., D.R. Hanson, and C.J. Howard, Reactions of SF_6 and I^- with atmospheric gases, *J. Phys. Chem.*, **99**, 5001-5008, 1995.
- Jaegle, L., Y.L. Yung, G.C. Toon, B. Sen, and J.F. Wavner, Balloon observations of organic and inorganic chlorine in the stratosphere: The role of HClO_4 production on sulfate aerosols, *Geophys. Res. Lett.*, **23**, 1749-1752, 1996.
- Kames, J., S. Schweighoefer, and U. Schurath, Henry's law constant and hydrolysis of peroxyacetyl nitrate (PAN), *J. Atmos. Chem.*, **12**, 169-180, 1991.
- Kames, J., and U. Schurath, Henry's law and hydrolysis-rate constants for peroxyacetyl nitrate (PAN) using a homogeneous gas-phase source, *J. Atmos. Chem.*, **21**, 151-164, 1995.
- Kasibhatla, P. S., H. Levy II, and W.J. Moxim, Global NO_x , HNO_3 , PAN, and NO_y distributions from fossil-fuel combustion emissions: A model study, *J. Geophys. Res.*, **98**, 7165-7180, 1993.
- Kasting, J.F., and H.B. Singh, Nonmethane hydrocarbons in the troposphere: impact on the odd hydrogen and odd nitrogen chemistry, *J. Geophys. Res.*, **91**, 13,239-13,256, 1986.
- Kleindienst, T. E., Recent developments in the chemistry and biology of peroxyacetyl nitrate, *Res. Chem. Intermed.*, **20**, 335-384, 1994.
- Kolb, C. E., et al., Laboratory studies of atmospheric heterogeneous chemistry, in *Current Problems in Atmospheric Chemistry*, J. R. Barker, Ed., *Adv. Phys. Chem.*, World Scientific Publishing Company, Inc., 1995.
- Langer, S., I. Wangberg, and E. Ljungstrom, Heterogeneous transformation of peroxyacetyl nitrate, *Atmos. Environ.*, **26A**, 3089-3098, 1992.
- Lee, Y. N., Kinetics of some aqueous-phase reactions of peroxyacetyl nitrate, in *Gaseous-Liquid*

- Chemistry of Natural Water*, BNL 51757, 21/1-21/7, Brookhaven National Laboratory, Brookhaven, NY, 1984.
- Leu, M. T., et al., Heterogeneous reactions of $\text{NO}_3(\text{g}) + \text{NaCl}(\text{s}) \rightarrow \text{HCl}(\text{g}) + \text{NaNO}_3(\text{s})$ and $\text{N}_2\text{O}_5(\text{g}) + \text{NaCl}(\text{s}) \rightarrow \text{ClNO}_2 + \text{NaNO}_3(\text{s})$, *J. Phys. Chem.*, 99, 13,203-13,212, 1995.
- Luo, B.P., et al., HCl volatility and liquid diffusion in aqueous sulfuric acid under stratospheric conditions, *Geophys. Res. Lett.*, 21, 49-52, 1994.
- Marrero, T.R., and E.A. Mason, Gaseous phase diffusion coefficients, *J. Phys. Chem. Ref. Data*, 1, 3-118, 1972,
- Mazely, T. L., R.R. Friedl, and S.P. Sander, Production of NO_2 from photolysis of peroxyacetyl nitrate, *J. Phys. Chem.*, 99, 8162-8169, 1995.
- Motz, H., and H. Wise, Diffusion and heterogeneous reactions. 111. Atom recombination at a catalytic boundary, *J. Chem. Phys.*, 32, 1893-1894, 1960.
- Nicksic, S. W., J. Harkins, and P.K. Mueller, Some analyses of PAN and studies of its structure, *Atmos. Environ.*, 1, 11-18, 1967.
- Orlando, J. J., G.S. Tyndall, and J.G. Calvert, Thermal-deposition pathways for peroxyacetyl nitrate (PAN): Implications for atmospheric methyl nitrate levels, *Atmos. Environ.*, 26A, 3111-3118, 1992,
- Parrish, D. D., et al., indications of photochemical histories of Pacific air masses from measurements of atmospheric trace species at Point-Arena, California, *J. Geophys. Res.*, 97, 15,883-15,901, 1992.
- Ridley, B. A., et al., Ratios of peroxyacetyl nitrate to active nitrogen observed during aircraft flights over the Eastern Pacific Ocean and continental United States, *J. Geophys. Res.*, 95, 10,179-10,192, 1990.
- Roberts, J. M., and S.B. Bertman, The thermal-decomposition of peroxyacetyl nitrate (PAN) and peroxyacetylnitric anhydride (MPAN), *Int. J. Chem. Kinet.*, 24, 297-307, 1992.
- Singh, H. B., and P.L. Hanst, Peroxyacetyl nitrate (PAN) in the unpolluted atmosphere: An important reservoir for nitrogen oxides, *Geophys. Res. Lett.*, 8, 941-944, 1981.
- Singh, H.B., L.J. Salas, and W. Viezee, Global distribution of peroxyacetyl nitrate, *Nature*, 321, 588-591, 1986,
- Singh, H. B., et al., Peroxyacetyl nitrate measurements during CITE 2: Atmospheric distribution

- and precursor relationships, *J. Geophys. Res.*, **95**, 10,163-10,178, 1990.
- Singh, H.B. et al., Atmospheric measurements of peroxyacetyl nitrate and other organic nitrate at high latitudes: Possible sources and sinks, *J. Geophys. Res.*, **97**, 16,511-16,522, 1992.
- Spicer, C. W., G.M. Sverdrup, and M.R. Kuhlman, Smog chamber studies of NO_x chemistry in power plant plumes, *Atmos. Environ.*, **15**, 2353-2365, 1981.
- Stephens, F.R., P. I. Hanst, R. C. Doerr, and W. Ii. Scott, Reactions of nitrogen dioxide and organic compounds in air, *Ind. Eng. Chem.*, **48**, 1498-1504, 1956.
- Stephens, F.R., The formation, reactions, and properties of peroxyacetyl nitrate (PAN's) in photochemical air pollution, *Adv. Environ. Sci.*, **1**, 119-146, 1969.
- Stepson, P.B., D.R. Hastie, K.W. So, and H.J. Schiff, Relationships between PAN, PPN, and O_3 at urban and rural sites in Ontario, *Atmos. Environ.*, **26A**, 1259-1270, 1992.
- Talukdar, R. K., et al., Investigation of the loss process for peroxyacetyl nitrate in the atmosphere: UV photolysis and reaction with OH, *J. Geophys. Res.*, **100**, 14,163-14,173, 1995.
- Watson, L. R., et al., Uptake of I-ICI molecules by aqueous sulfuric acid droplets as a function of acid concentrate ion, *J. Geophys. Res.*, **95**, 5631-5638, 1990.
- Schwartz, S. E., Mass-transport considerations pertinent to aqueous phase reactions of gases in liquid-water, in *Chemistry of Multiphase Atmospheric System*; Jaeschke, W., Ed., NATO ASI Series, Vol. G6, NATO, Brussels, 1986.
- Williams, L.R., and F.S. Long, Viscosity of supercooled sulfuric acid solutions, *J. Phys. Chem.*, **99**, 3748-3751, 1995.
- Worsnop, D. R., et al., Temperature dependence of mass accommodation ion of SO_2 and H_2O_2 on aqueous surfaces, *J. Phys. Chem.*, **93**, 1159-1172, 1989.
- Zhang, R., P.J. Wooldridge, J. P. Il. Abbatt, and M.J. Molina, Physical chemistry of the $\text{H}_2\text{SO}_4/\text{H}_2\text{O}$ binary system at low temperatures: Stratospheric implications, *J. Phys. Chem.*, **97**, 7351-7358, 1993.
- Zhang, R., M.T. Leu, and L.F. Keyser, Heterogeneous reactions of ClONO_2 , HCl, and HOCl on liquid sulfuric acid surfaces, *J. Phys. Chem.*, **98**, 13,563-13,574, 1994.
- Zhang, R., M.T. Leu, and L.F. Keyser, Heterogeneous chemistry of HONO on liquid sulfuric acid: A new mechanism of chlorine activation on stratospheric sulfate aerosols, *J. Phys. Chem.*, **100**, 339-345, 1996.

Table 1, Measured Values of $H^* \sqrt{D_t}$ and H^* for PAN in Liquid H_2SO_4 Solutions

H_2SO_4 Content (W t %)	Temperature (K)	$H^* \sqrt{D_t}$ ($M atm^{-1} cm s^{1/2}$)	H^* ($M atm^{-1}$)
46	199.1	7.20	6.47×10^4
	199.1	7.40	6.65×10^4
	202.3	5.80	4.17×10^4
	207.2	4.28	2.28×10^4
	211.2	2.79	1.20×10^4
	216.5	1.66	5.54×10^3
54	207.8	3.10	2.00×10^4
	208.2	3.00	1.89×10^4
	213.8	2.25	1.05×10^4
	214.9	2.01	8.85×10^3
	216.5	1.05	4.27×10^3
	216.8	1.12	4.50×10^3
	219.4	0.65	2.32×10^3
	226.0	0.32	8.75×10^2
59	207.8	3.12	2.42×10^4
	208.9	3.12	2.26×10^4
	209.6	3.00	2.08×10^4
	211.5	2.71	1.68×10^4
	212.8	2.15	1.24×10^4
	214.7	1.57	8.17×10^3
	216.6	0.85	4.01×10^3
	207.8	2.22	5.58×10^4
72	208.0	2.11	5.14×10^4
	208.1	2.12	5.22×10^4
	211.7	2.01	3.34×10^4
	212.6	1.80	2.88×10^4
	213.4	1.36	2.03×10^4
	214.8	1.05	1.40×10^4
	217.0	0.82	9.24×10^3
	219.2	0.60	5.77×10^3
	221.6	0.38	3.13×10^3

Figure Captions

- Figure 1. Mass spectra of He^+ , O_2^+ , and H_3O^+ reagent ions and O_2^+ reaction with the effluent from a PAN bubbler. PAN is detected as CH_3CO^+ ($m/e = 43$) or NO_2^+ ($m/e = 46$). In Fig. 1a, a small, yet distinguishable peak at $m/e = 8$ is due to the He_2^+ ions.
- Figure 2. Variation of the PAN signal as a function of time. PAN was exposed to a sulfuric acid film of 30 cm in length at 1.2 min and the exposure was terminated at 3.4 min. The temperature of the flow reactor was held at 212 K and the acid content of the film was estimated to be - 59 wt %. Experimental conditions are: $P_{\text{He}} = 0.42$ Torr, $V \approx 1800$ cm s⁻¹, and $P_{\text{PAN}} \approx 8 \times 10^{-7}$ Torr.
- Figure 3. Calculated time-dependent uptake coefficients as a function of $t^{1/2}$ of data displayed in Figure 2. The solid straight line is a linear least squares fit through the data. The slope of the line is used to extract the quantity $H^* \sqrt{D_l}$.
- Figure 4. Measured values of $H^* \sqrt{D_l}$ against the reciprocal of temperature for various H_2SO_4 contents: (○) 46 wt %; (○) 54 wt %; (V,) 59 wt %; (▼) 72 wt %. Experimental conditions are: $P_{\text{He}} = 0.40$ to 0.45 Torr, $V = 1600$ to 2000 cm s⁻¹, and $P_{\text{PAN}} \approx 10^{-7}$ to 10^{-6} Torr.
- Figure 5, Calculated H^* for data displayed in Figure 4 by estimating the liquid-phase diffusion coefficient using the cubic cell model. The different symbols correspond to different H_2SO_4 contents: (○) 46 wt %; (.) 54 wt %; (∇) 59 wt %; (▼) 72 wt %. The dashed line represents the Henry's solubility constants extrapolated to low temperatures based on the work of Kames et al. [1991] and Kames and Schurath [1995].

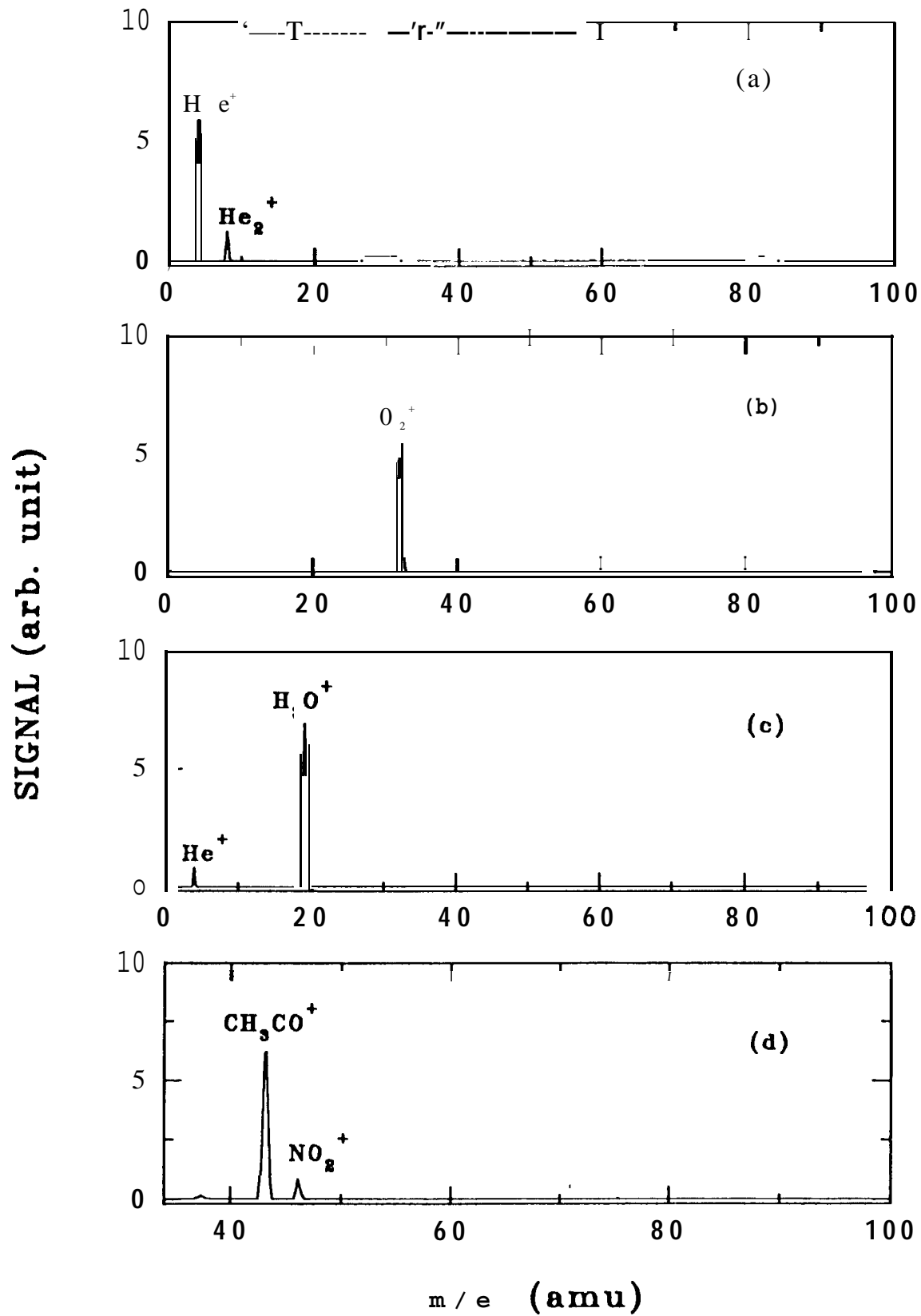


Fig. 1

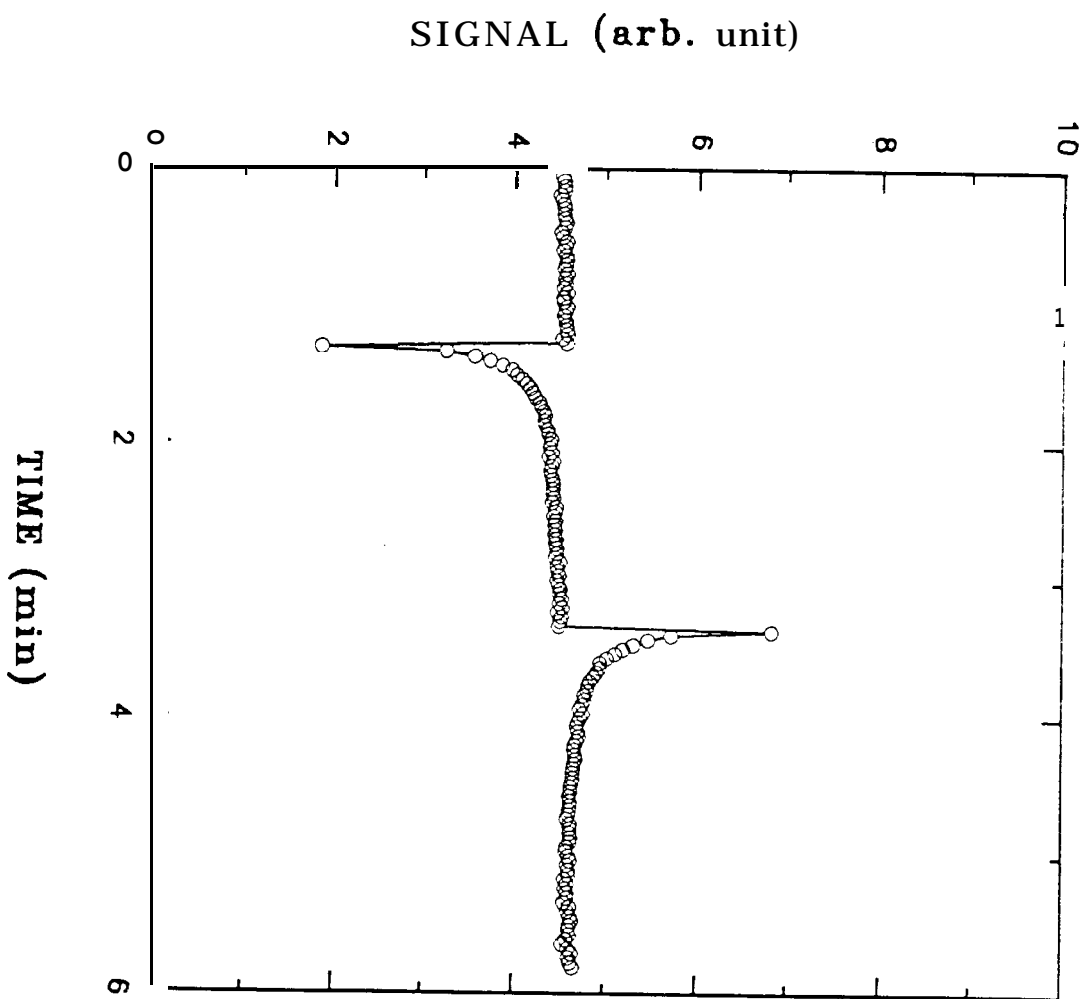


Fig 2

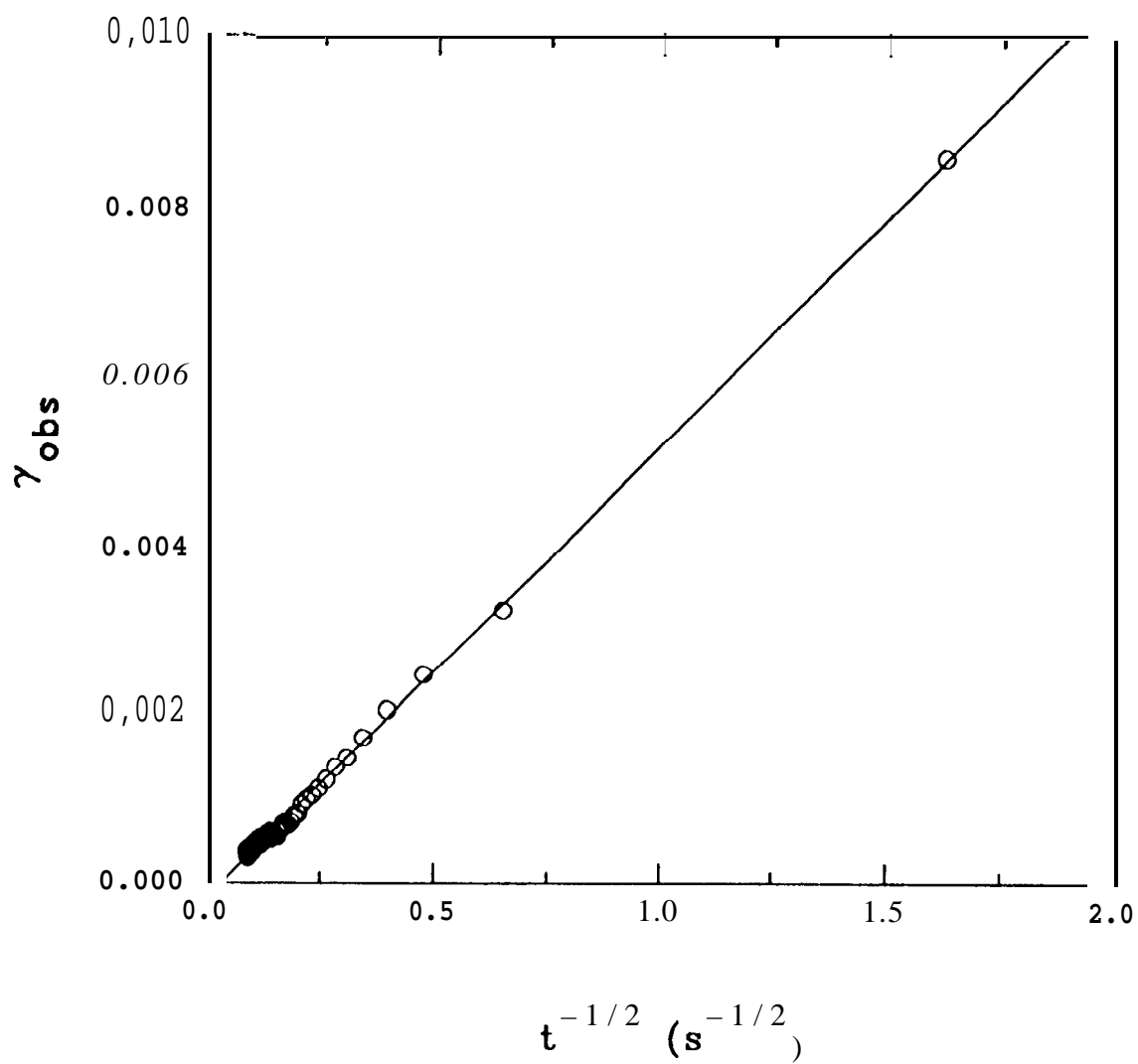


Fig. 3

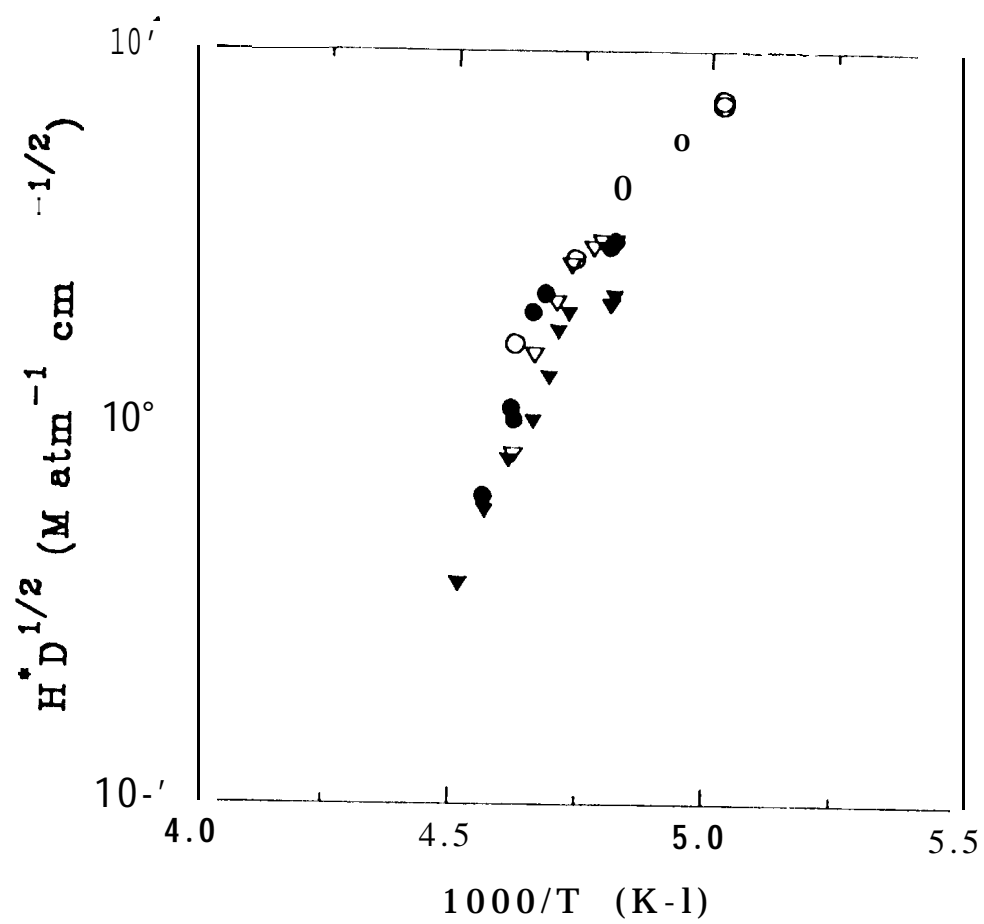


Fig. 4

